IRRADIATION DAMAGE STUDIES OF HIGH POWER ACCELERATOR MATERIALS

Nicholas Simos[1], H.G. Kirk, P. Thieberger, H. Ludewig, P-T Trung, J. O Conor, L. Mausner, K.T. McDonald, K. Yoshimura, J.R.J. Bennett

Corresponding author:

Nicholas Simos
Brookhaven National Laboratory
Upton, NY 11973
(E-mail: simos@bnl.gov, telephone: 631-344-7229, fax: 631 344-7650)

IRRADIATION DAMAGE STUDIES OF HIGH-POWER ACCELERATOR MATERIALS

N. Simos[1*], H. Kirk, P. Thieberger, H. Ludewig, J. O Conor[1], L. Mausner[1], P.T. Trung[2],

K.T. McDonald[3], K. Yoshimura[4], J.R.J. Bennett[5]

[1]Brookhaven National Laboratory, Upton, NY 11973, USA
[2]SUNY Stony Brook, NY 11794 , USA
[3]Princeton University, Princeton, NJ 08544, USA
[4]KEK, 1-1 Oho, Tsukuba, Ibaraki 305-0801, Japan
[5]Rutherford Appleton Laboratory, CCLRC, Chilton, Didcot, OX11 0QX, UK

ABSTRACT:

High-performance production targets and other critical accelerator components intercepting intense, energetic proton beams are essential as the accelerator community envisions the next generation, multi-MW accelerators. Materials that have served the nuclear sector well may not be suitable to play such a role which demands that the material comprising the beam-intercepting element must, in addition to the long exposure which leads to accumulated irradiation damage, also endure short exposure that manifests itself as thermo-mechanical shock. The ability of materials to resist irradiation-induced degradation of its properties that control shock and fatigue is of primary interest. The need for such materials that extend beyond resistance to the neutron-driven irradiation damage of reactor components has led to an extensive search and experimentation with new alloys and composites. These new high-performance materials, which appear to possess the right combination of mechanical and physical properties, are explored through a multi-phased experimental study at Brookhaven National Laboratory (BNL). This study, which brings together the interest in accelerator targets of different facilities around the world, seeks to simulate conditions of both short and long exposure to proton beams to assess the survivability potential of these new alloys and

composite materials. While thermo-mechanical shock effects have been studied in the early stages of this comprehensive effort, it is irradiation damage that is currently the focus of the study and results to-date are presented in this paper along with the status and objectives of on-going studies. Of special interest are results depicting damage reversal through post-irradiation annealing in some of the materials. High fluences of 200 and/or 117 MeV protons provided by the BNL Linac beam that serves the Isotope Production Facility were used to assess irradiation damage in these new composites and alloys.

KEYWORDS: Accelerator, target, irradiation, damage, annealing

---

Introduction

With the ever-increasing accelerator power required to support high–energy physics initiatives, the pool of materials forming production targets or other critical components capable to withstand the pulse intensities associated with these multi-MW class machines is minimized. MW-class accelerator targets, in addition to the high proton fluences they must endure during their operational life, fluences that may approach those of reactor-based materials typically exposed to high neutron fluxes, must be able to continuously absorb and diffuse the severe thermo-mechanical shock resulting from the intense proton pulses. Tightly focused, high-energy proton pulses must be intercepted by the envisioned accelerator targets within several nanoseconds leading to instantaneous fluxes of the order of 10^{24} protons/cm^2/s. Densities of energy deposited under these conditions on the target as well as other beam-intercepting elements like collimators are estimated to be extremely high and far beyond what common materials, even those with extensive reactor-based track record, can tolerate. Further, the thermo-mechanical fatigue issue, direct result of the pulsed nature of these MW-class accelerators, adds additional performance requirements on these materials because of the need to extend the operational life of these components. Fatigue limits, even under the best of circumstances in which materials can resist irradiation-induced degradation of their properties, can be reached in short time given that accelerator pulse frequencies can reach 60 Hz.

The need to identify materials that go beyond the neutron-driven irradiation damage of reactor components and are able to tolerate severe beam-induced shock has led to an extensive search and experimentation with new alloys and composites. These new high-performance materials,

which, in the absence of irradiation exposure, appear to possess the right combination of mechanical and physical properties, are explored through a multi-phased experimental study at Brookhaven National Laboratory (BNL). During the first phase of the study target and beam-window materials were exposed to 24 GeV, high-intensity proton pulses provided at the BNL Alternating Gradient Synchrotron (AGS). The objectives of this study [Ref. 4] was to assess how carbon composites and other super-alloys respond to the beam-induced shock and whether prediction of their response is possible based on simulation models. The latter is an essential element towards achieving the ultimate goal of multi-MW beam intensities. Verification of the ability to predict shock response at intensity levels the current accelerators can provide will form the foundation for extrapolating the understanding to the MW-class accelerators that are being conceptualized. While it is desirable to induce beam shock conditions on materials that have experienced cumulative degradation of their properties as a result of prolonged exposure, a condition that exactly simulates what the real target materials will experience in MW-class accelerators, facilities capable of delivering both aspects of "damage" simultaneously are currently unavailable. Therefore, this study, as well as other relevant studies being pursued, while relying on addressing the two components separately, attempt to inch ever closer to the desired state that can only be delivered by the multi-MW accelerator that is in its conceptual state. In this paper, the results of the BNL shock studies will be mentioned briefly since they have been reported in prior reports [Ref. 1, 2, 3 and 4]. Instead the focus will be on the aspects of the experimental study that address the effects of irradiation on the material properties of new alloys and composites that are pertinent to their performance as targets and other beam-intercepting accelerator elements.

While a wealth of relevant material damage data, even on materials that may be considered to play roles other than targets in high-power accelerators, is available to the accelerator community from reactor studies and experience data [Ref. 5] this information is almost entirely linked to neutron exposure damage effects on these materials. The correlation between prolonged neutron and proton exposure effects is still too incomplete to allow for direct use of the reactor-based data to proton accelerators. In addition, irradiation damage data from either neutrons or protons for the recently developed "smart" alloys and composites, which hold most of the promise, are either scarce or non-existent.

The irradiation damage effort that is the focus of this paper has been conducted in a series of phases. During the first phase of the study inconel-718 and super-invar where irradiated using the 200 MeV protons of the Brookhaven Linac Isotope Producer (BLIP). The primary objective was to primarily assess how the extremely low thermal expansion coefficient (CTE) of super-invar survives prolonged exposure to protons. CTE is one of the physical properties that play a pivotal role in determining the state of thermal stress in the material following interception of proton pulses. A low CTE is desirable, since the generated stress is proportional to it and the question is whether irradiation induces significant changes in its unirradiated value.   The study of inconel-718, although of secondary interest, was to confirm that the material is stable regarding its reported [6] stable CTE under irradiation conditions. The damage levels achieved during this first phase were approximately 0.25 displacements-per-atom (dpa) for super invar and approximately 0.05 dpa for inconel-718. Results of irradiation-induced changes on the two materials are presented in this paper.

In the second phase of study, the search for new alloys, composites and "smart" materials continued and a new and expanded matrix was established. It included materials in the low-Z and mid-Z regimes in an effort to satisfy accelerator initiative needs that are linked to the atomic number of the target material. Specifically, the low-Z regime was comprised by the three-dimensional (3D) weaved carbon-carbon composite, graphite grade IG-43, alloy (or even termed composite) AlBeMet (62% beryllium and 38% aluminum), and pure beryllium. The mid-Z regime included the titanium alloy Ti-6Al-4V, an annealed version of the super-alloy "gum" metal, and Vascomax-350. In addition, nickel-plated aluminum samples were introduced in the irradiation matrix to study the combined effects of irradiation and corrosive environment on this special plating. A dedicated study on the effects of proton irradiation on the two-dimensional (2D) carbon-carbon composite structure was also conducted. Assessment of the structural integrity of this particular composite and its ability to maintain low CTE were the primary objectives.

Most recently, a new phase of the study has been launched in an effort to address some of the issues that resulted from the previous phases and to achieve higher exposure. Some of the already tested materials were re-introduced into the matrix along with all new materials such as the "cold-worked" gum metal, copper, glidcop and the high-Z materials tungsten and tantalum. Noteworthy is the re-introduction of post-irradiation annealed super-invar into the matrix to assess the response to re-exposure of materials that have undergone annealing. While the irradiation portion of the last phase has been completed after approximately doubling the damage of phase two, the post-irradiation analysis is still pending. Results and discussion on the new findings will be reported in a follow-up report.

Experimental Effort

Irradiation Facility and Proton Beam

Shown in Figure 1 is a schematic of the irradiation facility where materials are exposed to protons. The 117 or 200 MeV proton beam at the end of the Linac is directed toward the isotope production facility where a special target station submerged in ~30 ft of water and with water flowing through the assemblies has been designed and installed. The operation normally shares the beam with the accelerator complex (Booster-AGS-RHIC) in a mode that allows six out of the seven pulses of protons to be directed toward the isotope or irradiation targets. As shown in Figure 1, the typical beam current is 80 µA with some fluctuation around this nominal value. During the various irradiation phases beam current as high as 95 µA were seen. The proton beam is purposely de-focused in order to expose as much as possible of the volume of the special targets used for harvesting isotopes. Special nickel foils integrated into the irradiation assemblies help establish the beam spot size, shape and location during irradiation. Beam spot sizes with full width at half maximum (FWHM) ≈ 15mm are typical.

Test Set-up and Conditions

Figure 2 depicts one of packing arrangements used during irradiation of a material matrix. The requirement that the beam entering the assembly with 200 MeV must leave at a particular energy specified by the isotope production targets downstream makes the arrangement a serious challenge. Also required is that the Gaussian shape of the beam entering the irradiation target space must be maintained so that it does not affect the isotope production downstream. This requires a very special packing of the different planes of irradiated materials. Shown in Figure 3 are two of the types of specimens used during irradiation. One is used for the evaluation of the mechanical properties and the other for physical properties such as thermal expansion. Their particular shape has been chosen to satisfy the requirements

imposed by the isotope production. Figure 6 depicts an actual layer of these two types of specimens integrated to form a "gap-free" plane.

Since establishing the irradiating temperature is essential a special technique has been implemented in this study to help establish the thermo-hydraulic parameters. Specifically, to overcome the inaccessibility of the irradiation space when the beam is on, an indirect method relying on the thermal sensitive paint (TSP) was implemented. With this technique, plates painted with TSP and occupying the positions of the actual targets were exposed to the same beam. Heat transfer simulation helped establish the time of steady-state condition reached by the painted targets. Figure 4 depicts the actual aluminum plate-target exposed to the beam and the simulated temperature distribution expected. The TSP of the exposed target clearly establishes the temperature fringes induced by the beam. Based on simulations relying on detailed finite element modeling, the irradiation temperatures of the mid-Z materials have been estimated to be approximately 300 $^{\circ}$C with Vascomax experiencing slightly higher temperatures.

Post-irradiation analysis

Post-irradiation analysis of the materials exposed to the beam was performed at the BNL hot labs. Prior to the actual testing of the specimens for physical and mechanical property changes, the activation of specimens was measured and γ-spectroscopy was performed on a sample of specimens. The special nickel films positioned within the irradiation matrix were autoradiographed to establish the beam spot size, shape and position relative to the specimens. Figure 5 depicts an exposed nickel films and the resulting autoradiagraphy. In Figure 6 we show both the packing of one of the layers of material specimens and the relative position of the beam, deduced from the autoradiograph.

Also shown in Figure 6 is the approach used to generate the spatial distribution of the damage throughout the matrix of materials/specimens. Specifically, the zone of interest was finely subdivided and by using damage cross sections [Ref. 9] along with the MCNPX Monte Carlo Code [Ref. 8] and the irradiating beam position and shape, dpa values were estimated for each location.

The importance of the space discretization is in that the location of rupture in the tensile specimens can be correlated with the distribution of the damage along the gauge length. The analysis revealed that primarily the damage was the result of incident proton fluence. The contribution of neutrons to the damage was minimal.

Experimental Results

The post-irradiation analysis of the exposed material matrix was conducted in the BNL hot cell facility. Thermal expansion measurements using a LINSEIS dilatometer with nanometer-level sensitivity and stress-strain relations using a 5kN tensile testing apparatus (Tenius-Olsen) were made. The post-irradiation analysis was performed remotely from computers operating outside the two hot cells used.

Figures 7 and 8 depict the results of the first of the series of irradiation phases. The objective of the first phase was to assess how and if super-invar maintains its low CTE following prolonged proton exposure. Its low CTE was considered very attractive for proton target considerations because of its beneficial effect toward shock stresses. As seen in Figure 7 even modest exposure (up to 0.25 dpa) leads to a five-fold increase in CTE. It became apparent that irradiation removes the effects of treatments on the alloy that result in very low thermal expansion characteristics in the range of 0 to 150 ^{o}C. Inconel-718 thermal expansion measurements on the other hand reconfirmed [Ref. 6] that the material CTE remains stable under irradiation. Based on the results shown in Figure 7, super-invar was removed from the list of materials for further consideration. Recent results, however, on other materials such as carbon-composites, showing the reversal of "damage" through annealing, damage caused by irradiation and manifesting itself as increase in the low CTE exhibited by these materials, prompted the re-evaluation of super invar under similar annealing. The results of annealing on the irradiated material are shown in Figure 9. The process identified the temperature threshold (T > 600 ^{o}C) required for reversing the damage. To assess how re-exposure will affect the material behavior, annealed super-invar was introduced into the latest irradiation matrix. Several neutron-irradiation studies have suggested [Ref. 5] that damage in materials recovered after irradiation is accelerated when re-introduced to the same irradiation conditions. Post-

irradiation analysis of the recently re-exposed annealed super invar will focus on this particular issue.

Figure 10 depicts the changes in the CTE of several low-Z materials and composites as a function of the average proton fluence. Figure 10d represents the effects of post-irradiation annealing or thermal cycling on the 3-D carbon composite. Both the 2D and 3D weaved carbon composites exhibit negative CTEs for temperatures between 0 and 800 ^{o}C along the fiber reinforced planes. Manufacturer's data were reconfirmed for both materials in the course of this study. The onset of irradiation appears to dramatically alter the response of these composites. Thermal cycling, on the other hand, restores their peculiar, but very favorable negative CTE. Not shown in this paper is the recovery also exhibited by the 2D composite material in the direction normal to the fiber-reinforced planes. Concerns of structural degradation of these composites from very high fluences ($> 10^{20}$ p/cm^{2}) have prompted new irradiation damage studies that aim to achieve such fluences and rigorously examine the two composites. Figure 11 shows the CTE at 550 ^{o}C of Ti-6Al-4V, annealed gum metal and Vascomax (all mid-Z materials) as a function of the average proton fluence. Scattering of data is observed for Ti-6Al-4V and Vascomax at lower fluences. The CTE of the annealed gum metal, on the other hand, shows limited scattering between samples attributed probably to the special treatments the material was subjected to thus making it more homogeneous.

Figures 12 to 17 summarize post-irradiation results on the stress-strain relations of tested materials. Testing was conducted at room temperature and at different strain rates with most samples tested at 12.5 N/s rate. High strength, high-ductility and low elastic modulus are desirable properties to be both possessed and maintained during irradiation by the materials considered for accelerator targets and other critical beam-intercepting components like collimators. Figure 12 depicts stress strain results obtained from the study of super-invar. Loss

of ductility with simultaneous increase in yield strength is observed (also observed in neutron-irradiation studies of reactor materials). Knowing that the material has undergone special treatments to achieve, what is typical of the invar family, low thermal expansion, the un-irradiated material was heat treated to 300 and 500 ^{o}C and tested mechanically. As seen in Figure 12, heat treatment at 300 ^{o}C increased its strength and had no effect on the elastic modulus and ductility. Heat treatment at 500 ^{o}C, however, reduced the elastic modulus, reduced the strength and increased its ductility by making the material softer. Figure 13 shows stress-strain results of the titanium alloy Ti-6Al-4V as a function of irradiation damage in dpa. This strong alloy also exhibits the trend of ductility loss accompanied by strength increase. Figure 14 presents the stress-strain behavior of Vascomax-350 also as a function of irradiation damage. It is interesting to note that irradiation induces strength increase but the material maintains most of its ductility. It should be added that the irradiation temperature of Vascomax was slightly higher than that of the rest of the matrix (estimated to be ~350 ^{o}C). Further, the material surfaces exposed to the cooling water during irradiation experienced serious corrosion and that needs to be taken into consideration when assessing its viability as an accelerator target material where removing heat is essential. The stress-strain relation of the alloy (or composite) AlBeMet is shown in Figure 15. It is interesting to note, as in the case of Vascomax-350, that this material also resists loss of the ductility following irradiation. The effective low-Z of this material leads to significantly smaller dpa values as compared to the mid-Z counterparts.

Figure 16 depicts manufacturer's data on the alloy "gum" metal (Ti-12Ta-9Nb-3V-6Zr-O) exhibiting "super" properties in the un-irradiated state such as ultra-low elastic modulus, ultra-high strength, super plasticity and ultra-low expansion (invar-like behavior expanded to 400 ^{o}C). These properties are attributed to dislocation-free plastic deformations mechanisms

associated with elastic strain fields that range from nanometer scale to several tens of micrometers. As shown in Figure 16, the process of "cold-work" improves the material even further by lowering its elastic modulus, increasing its strength and its plastic deformation. Figure 16b depicts the thermal expansion and CTE of the cold-worked material as a function of temperature. It is interesting to note that the expanded range of the invar-like behavior is immediately followed by a narrow temperature band where dramatic increases in the CTE of the material are observed. Figure 17 presents stress-strain results on the annealed gum material obtained following proton exposure. The effect of irradiation damage on the super-ductility of the gum metal is evident. The material is unable to maintain any ductility even at relatively modest irradiation exposures. During the latest phase (ongoing) of the irradiation study, the cold-worked gum alloy was introduced into the matrix to assess how prone to radiation-induced embrittlement it is. Prior to irradiation, the cold-worked gum material was tested to establish the effects of temperature on the low CTE it exhibits in the range of 0-400 ^{o}C. As Figure 18 indicates, a single thermal cycle of peak temperature $T>550$ ^{o}C is able to remove the benefits of cold-working towards the low CTE exhibited by the cold-worked alloy.

Discussion

While an extensive database and experience on neutron irradiation damage exist as a result of the either operation of nuclear reactors or reactor-based experiments, there is still need a to assess new materials and alloys for accelerator applications. Although the reactor-based experience can provide significant insights regarding the manifestation of irradiation-induced damage in materials, a direct correlation between neutron and high energy proton exposures has yet to be fully established. An established link between the effects of the two species will allow the use of the wealth of neutron-based data in accelerator component long-term survivability associated with damage levels of the order of 100s of dpa achievable only during reactor operations. In the meantime, and driven by the need to assess how certain material properties that are more closely linked to accelerators rather than reactors (i.e. properties that control the state of shock in materials brought on by high intensity proton pulses), a search has been under way for new materials, super-alloys and composites that possess the right combination of properties. These materials have been put to the test of irradiation by exposing them to proton fluences that are, at least during the screening part of the effort, enough to indicate how prone are these materials to experiencing degradation of their properties.

The study thus far assessed damage in materials occupying the low-Z and mid-Z ranges. Special attention has been paid to carbon-carbon composites (both 2D and 3D configuration) as a potential replacement of graphite for beam targets and beam collimating elements. This was primarily prompted by the low thermal expansion properties of these composites which should result in much reduced shock response to proton pulses. The superiority of the composites in reducing shock was verified by beam-on-target experiments at BNL [Ref. 4]. What remains to be established, however, is the resilience of the carbon-based composites to radiation exposure anticipated during the operation of the envisioned multi-MW accelerators.

Preliminary results indicate that these composites may experience structural degradation at very high fluences. Irradiation studies addressing this issue continue and results will be made known in a follow-up report.

The irradiation damage studies described in this paper have shown that special alloys, such as super-invar, exhibit damage reversal through thermal annealing provided that certain temperature limits are exceeded. The possibility that materials, while being irradiated at high temperatures, as will be the case of beam intercepting targets, reverse the induced damage is very promising. Damage reversal through annealing or thermal cycling was also observed in both the 2D and 3D carbon composites.

Irradiation damage appeared to have a dramatic effect on the super-ductility of the annealed gum metal. This material that also exhibits low elastic modulus and high strength appears to maintain its strength well beyond the plastic limit of typical materials. Irradiation, however, causes severe embrittlement of the material even with modest exposure. Alloys such as Ti-6Al-4V, Vascomax-350 and AlBeMet experience loss of ductility with increased irradiation but the latter two show more resilience.

New irradiation studies are under way to assess (a) the damage potential in the carbon-carbon composites, (b) the effects of irradiation on the ductility and thermal expansion of the cold-worked gum metal, (c) the response of glidcop (0.15% aluminum, balance copper) to irradiation as compared to pure copper and especially in terms of thermal conductivity and CTE, (d) the degradation of the mechanical properties of tantalum and tungsten, including helium production and retention, and finally (e) the response of materials that experienced damage reversal through annealing (i.e. super-invar) to re-exposure. Results of the new study will be reported as they become available.

REFFERENCES

1. N. Simos, *et al.*, "*Experimental studies of targets and collimators for high intensity beams*," (to appear), ICFA-HB, 2006

2. N. Simos, *et al*., "Solid *Target Studies for Muon Colliders and Neutrino Beams*," Nucl. Phys. B (Proc. Suppl.) **155**, 288-290 (2006).

3. N. Simos, *et al*., "*Target Material Irradiation Studies for High-Intensity Accelerator Beams*," Nucl. Phys. B (Proc. Suppl.) **149**, 259-261 (2005).

4. H.G. Kirk, *et al.*, "Target Studies with BNL E951 at the AGS," Proc. 2001 PAC, (Chicago, IL, March 2001), p.1535.

5. *Primary Physical Effects*, Handbook

6. APT Materials Handbook, TPO-P00-MDD-X-00001, 20001.

7. K. Nishino, "Super Multifunctional Alloy "GUM METAL".Toyota CRDL., INC. Technical News.

8. MCNPX Users Manual-Version 2.1.5, L.S. Waters, ed., LANL, Los Alamos, NM. TPO-E83-GUG- X-00001. (1999)

9. E. Pitcher, LANL, "Material Damage Cross-Sections," Private Comm.
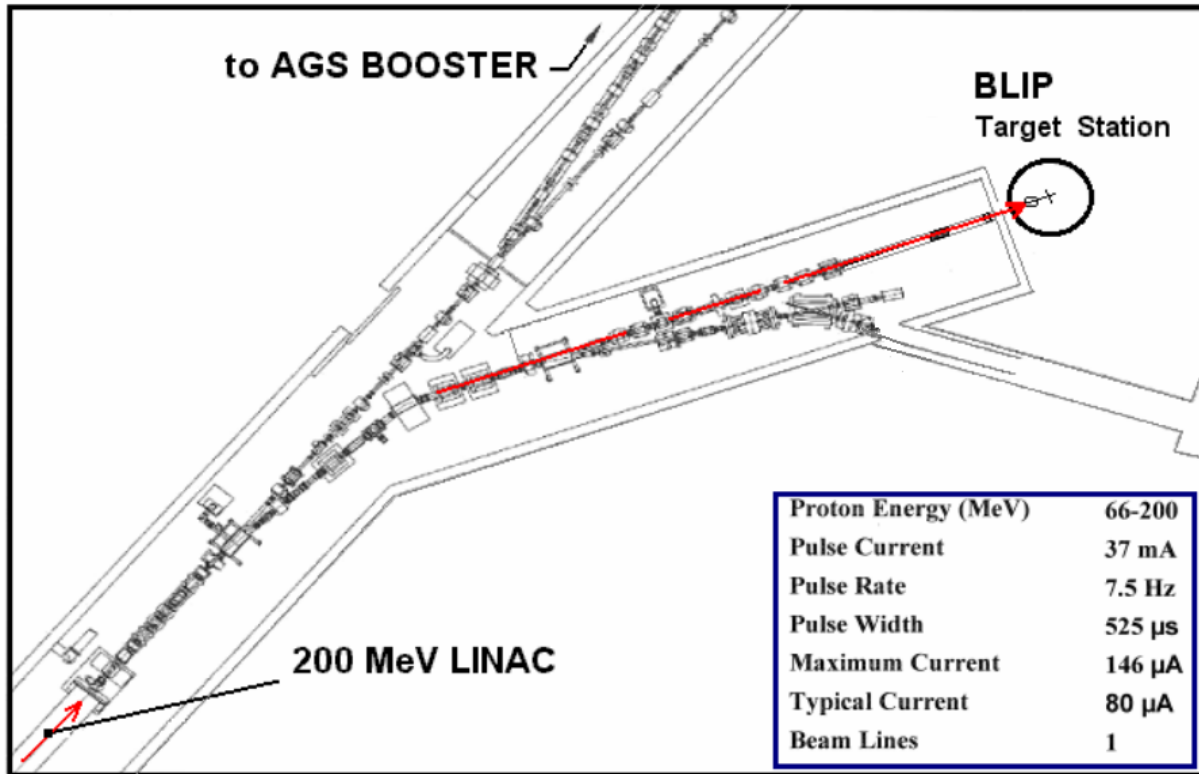
Figure 1: BNL experimental facilities used in the material irradiation study
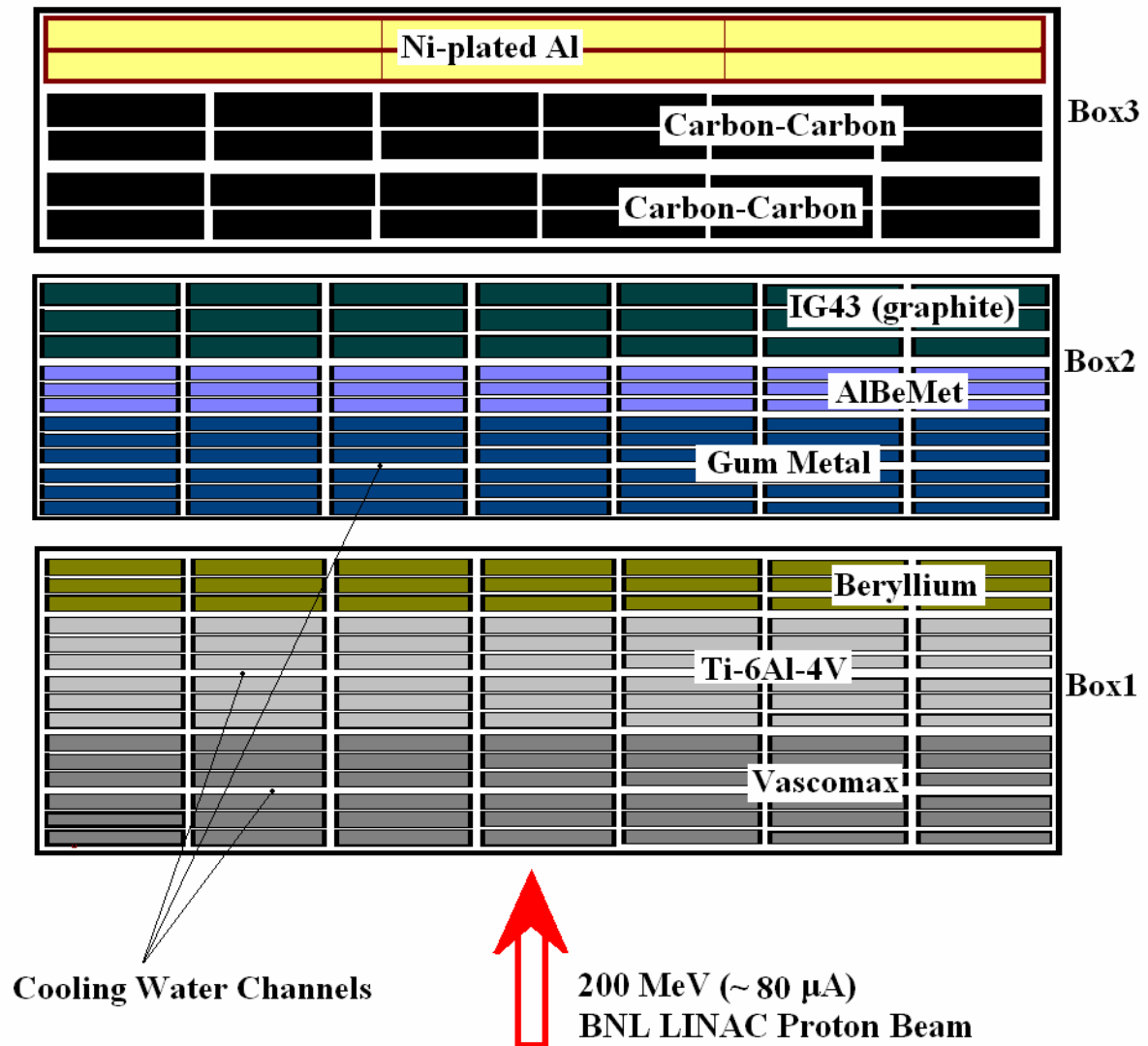
Figure 2: Specimen layout in the irradiation boxes used the BNL Phase II irradiation
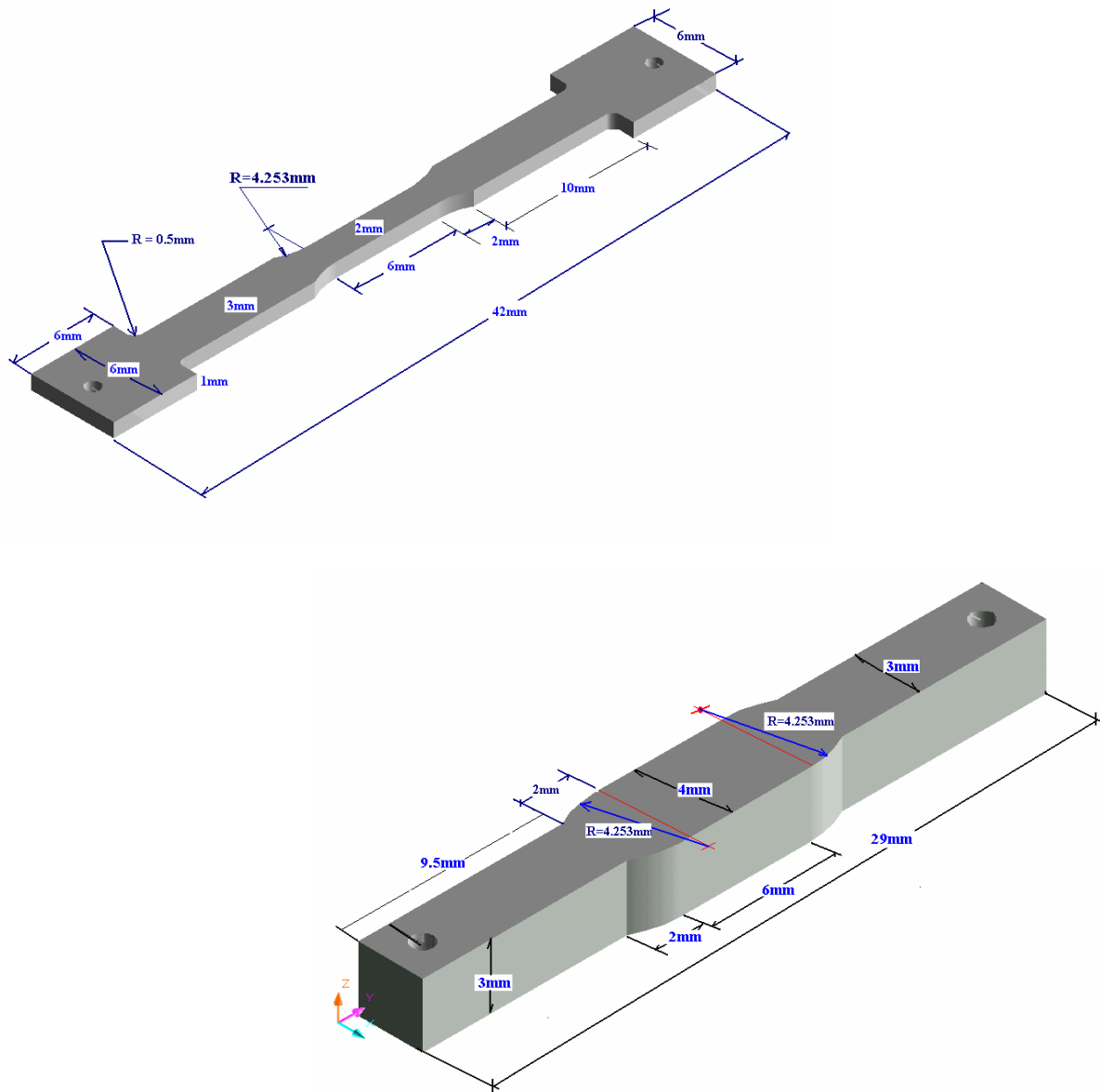
Figure 3: Specimen design for mechanical and physical property studies
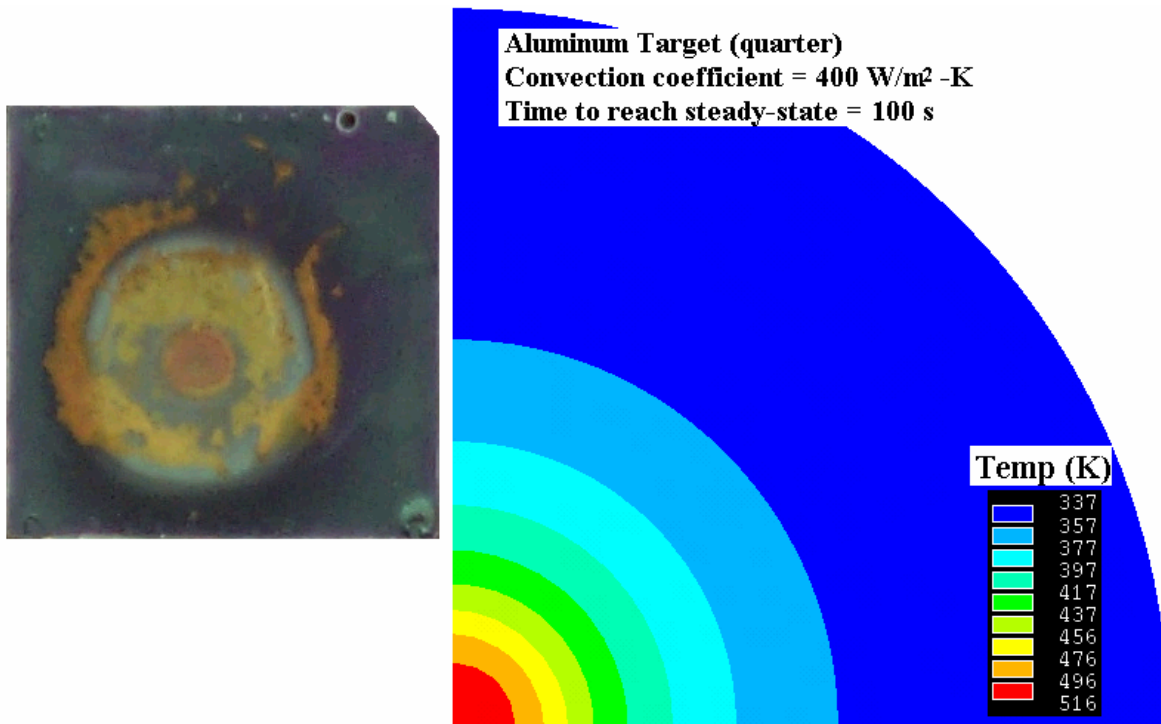
Figure 4: Irradiation temperature assessment during BNL BLIP operations. On the left the actual target "painted" with thermal sensitive paint (TSP) is shown following exposure to the beam and after reaching steady-state conditions. On the right are simulation results that helped benchmark the thermo-hydraulic parameters associated with the actual target irradiation set-up.
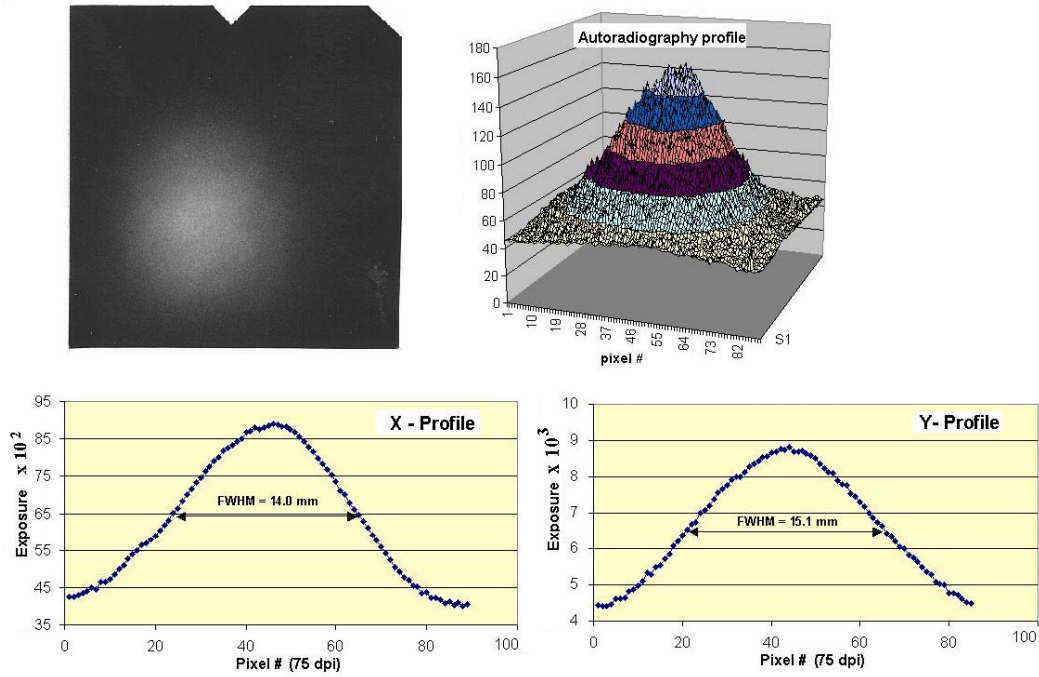
Figure 5: Autoradiography on embedded nickel films and assessment of proton beam profile
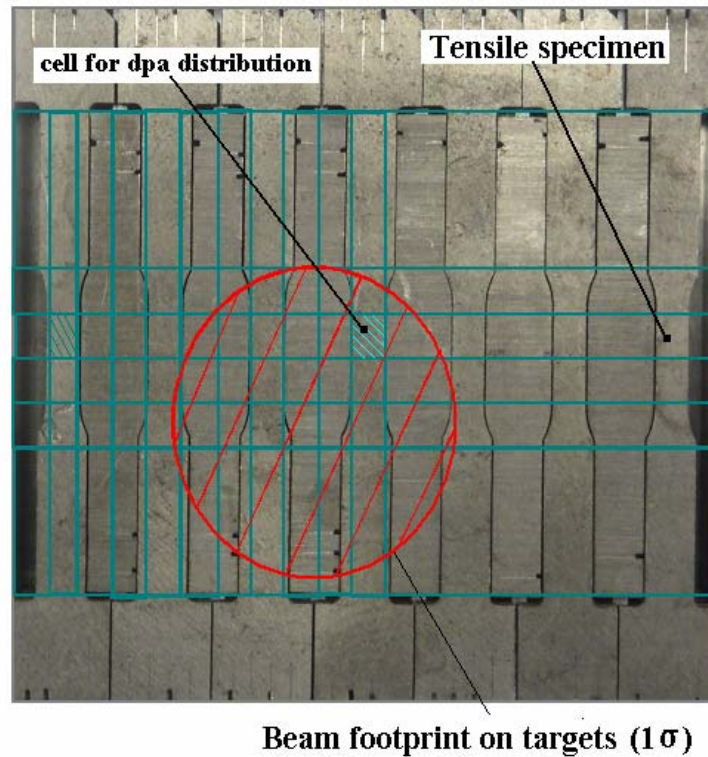
Figure 6: Integration of different types of specimens into the irradiation space. Also shown is the special numbering of the specimens used. Superimposed is the approximate location of the beam footprint and the discretization used for the spatial distribution of irradiation damage.
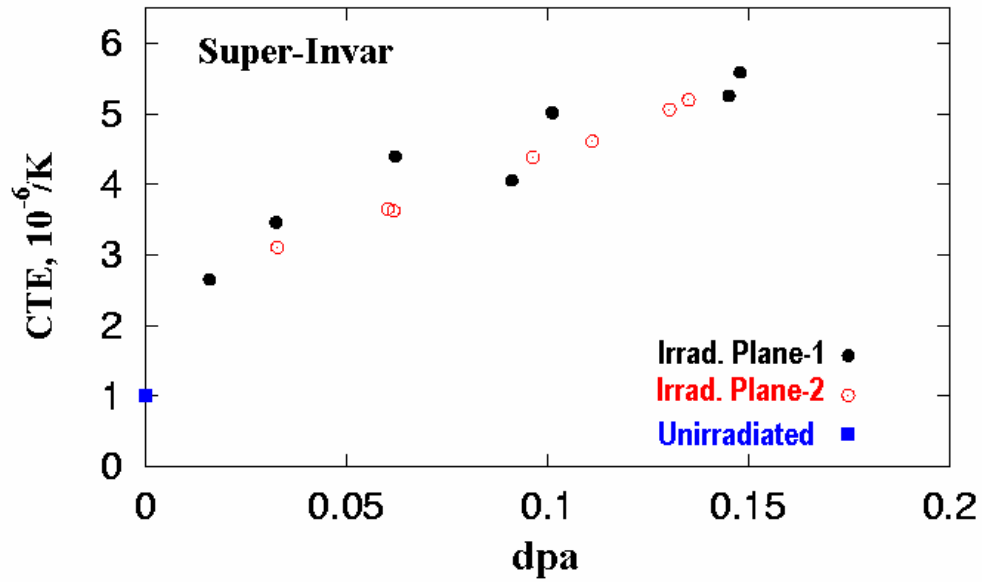
Figure 7: Effects of modest levels of irradiation damage on the thermal expansion coefficient (CTE) of super-invar.
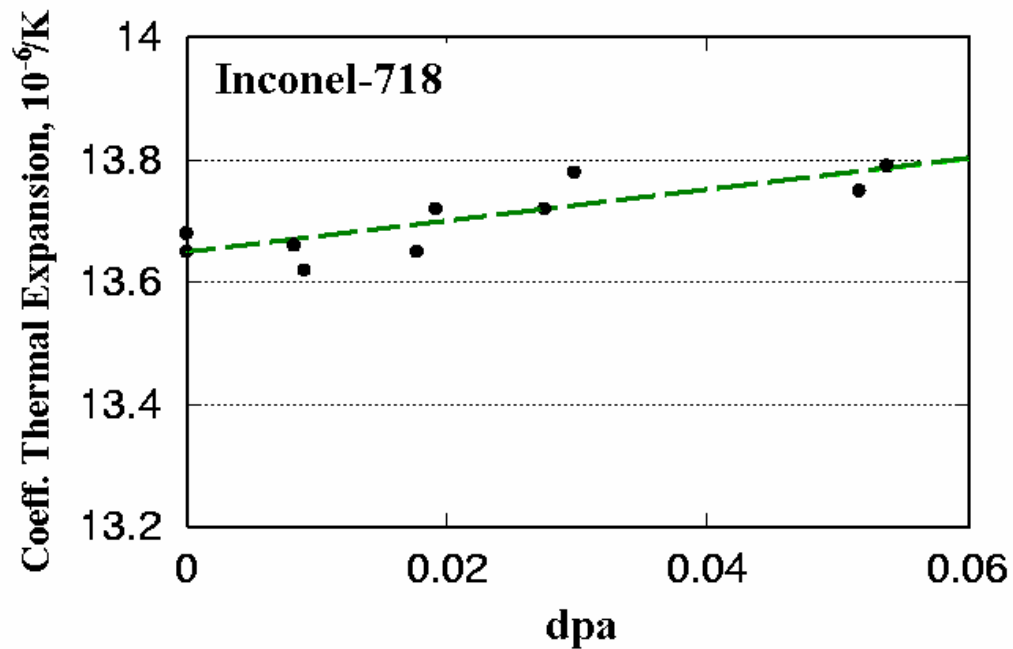
Figure 8: Proton irradiation effects on the CTE of Inconel-718. The very low dpa associated with inconel-718 is the result of its positioning near the edges of the irradiated plane.

(a)

(b)
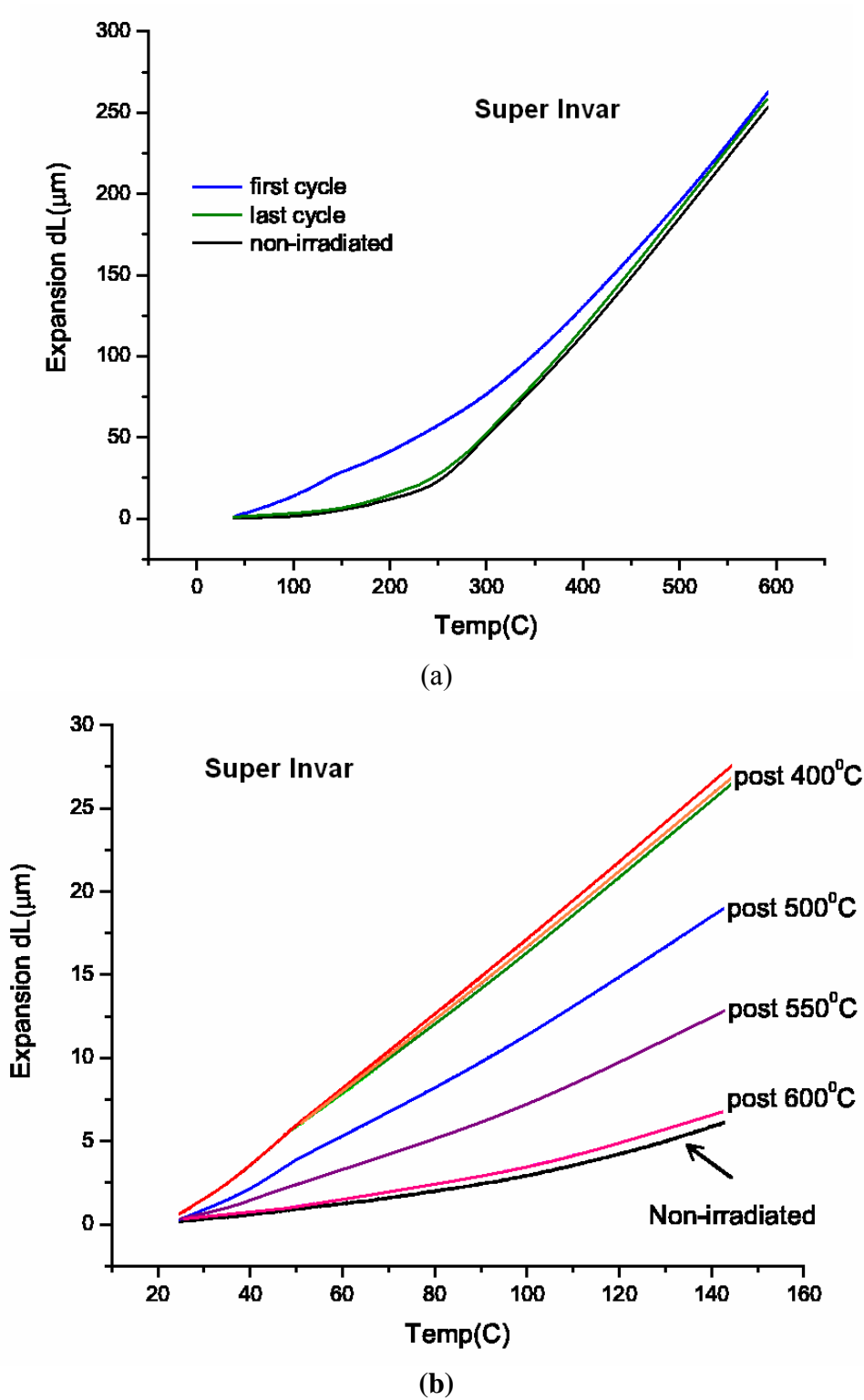
Figure 9: Effects of post-irradiation "annealing" on super invar. Thermal cycling with temperatures < 400 ^{o}C appear to have no effect towards reversing "damage" induced by protons. Thermal cycling with temperatures > 600 ^{o}C reverse the "damage" entirely.
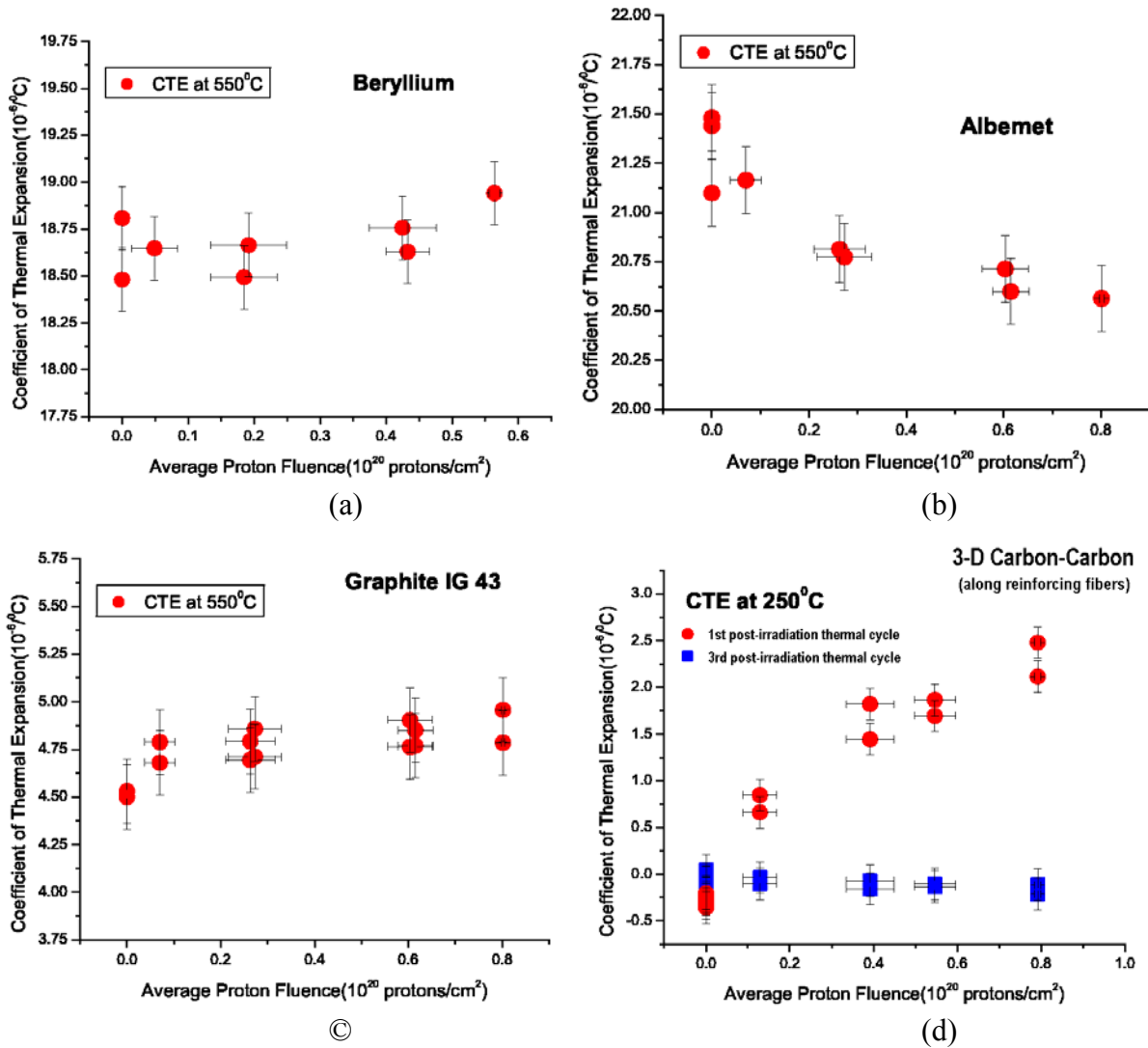
Figure 10: Irradiation effects on the CTE of several low-Z materials exposed to protons. The dramatic effects of irradiation on the CTE of the 3-D carbon composite and of the post-irradiation annealing through thermal cycling are evident in (d). Similar "annealing" behavior was observed in the 2-D carbon composite along the strong (fiber-reinforced) and the "weak" (normal to fiber planes) directions.
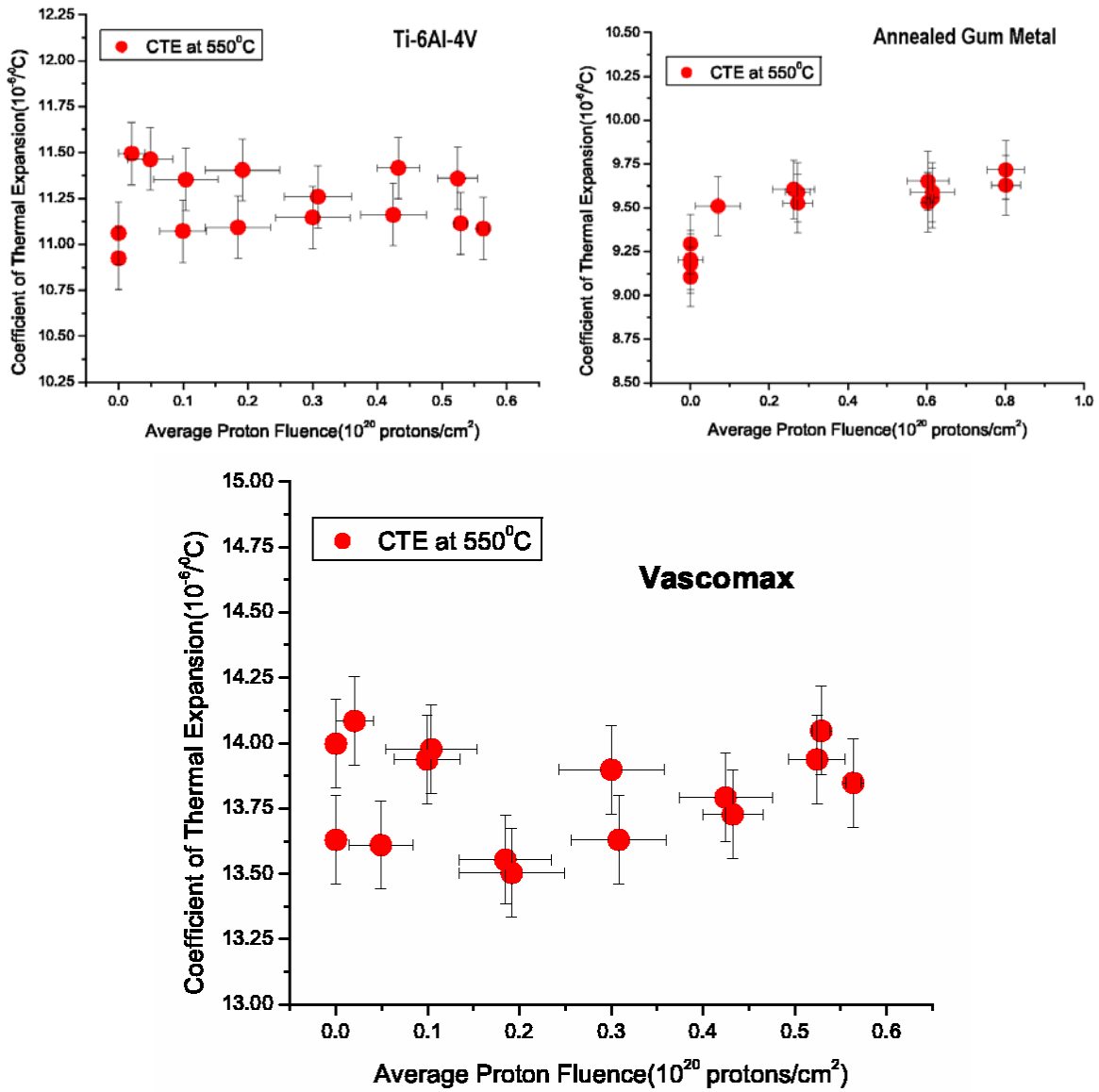
Figure 11: Irradiation effects on the CTE of several mid-Z materials exposed to protons.
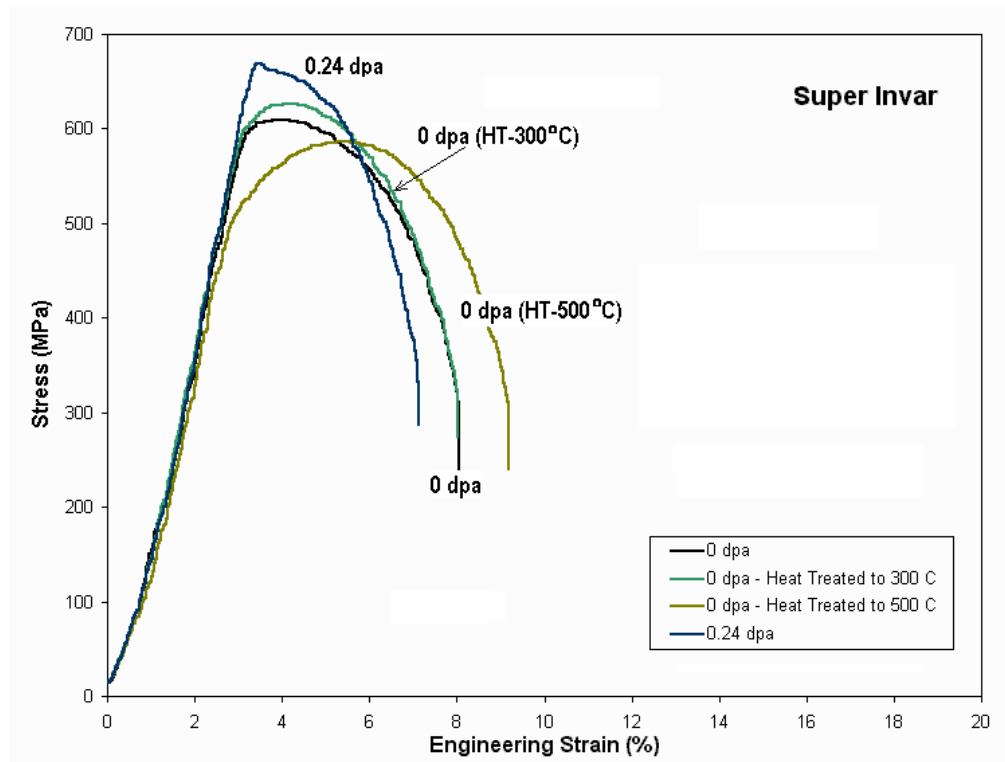
Figure 12: Irradiation and heat treatment effects on the stress-strain relation of super invar.
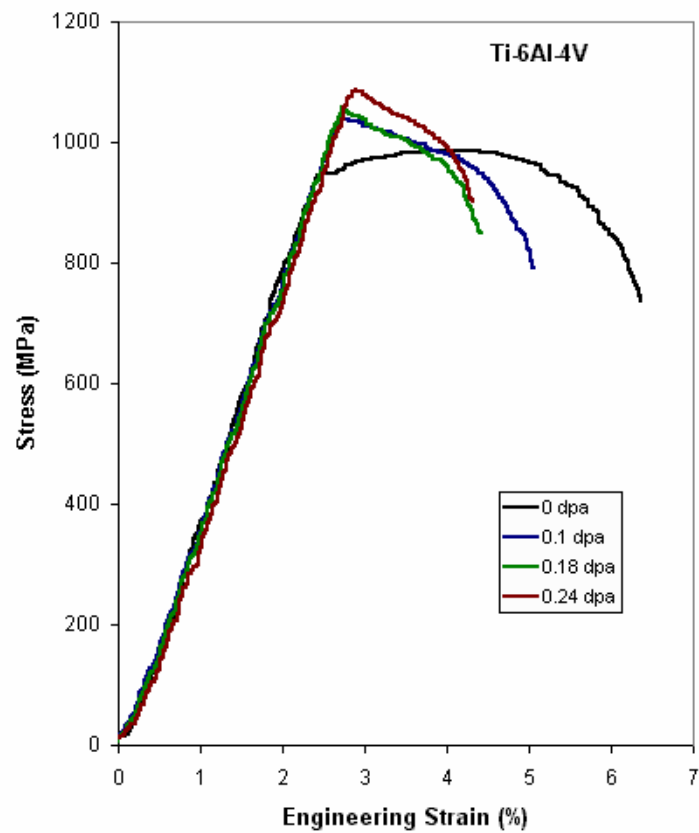
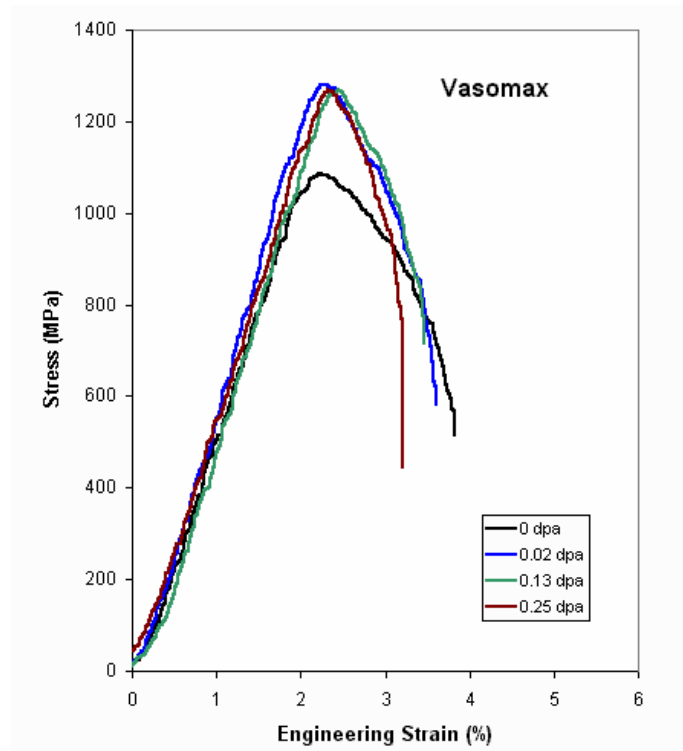**Figure 13**: Irradiation effects on the stress-strain relation of Ti-6Al-4V

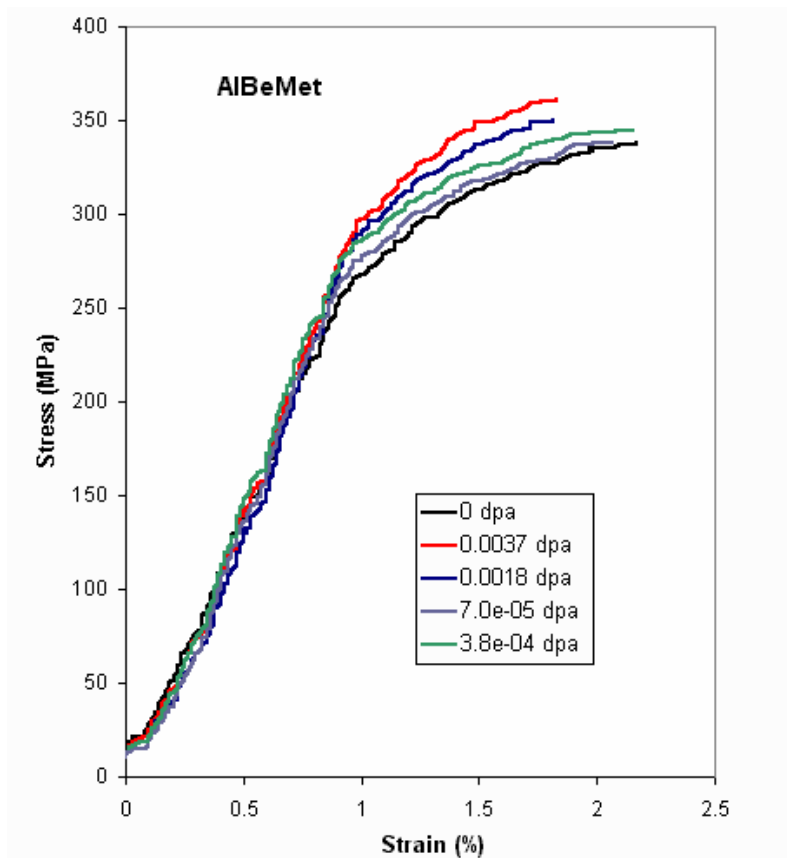**Figure 14**: Irradiation effects on the stress-strain relation of Vascomax-350

Figure 15: Irradiation effects on the stress-strain relation of the low-Z alloy AlBeMet (62% beryllium and 38% aluminum). Noteworthy is the retention of ductility exhibited by the alloy.
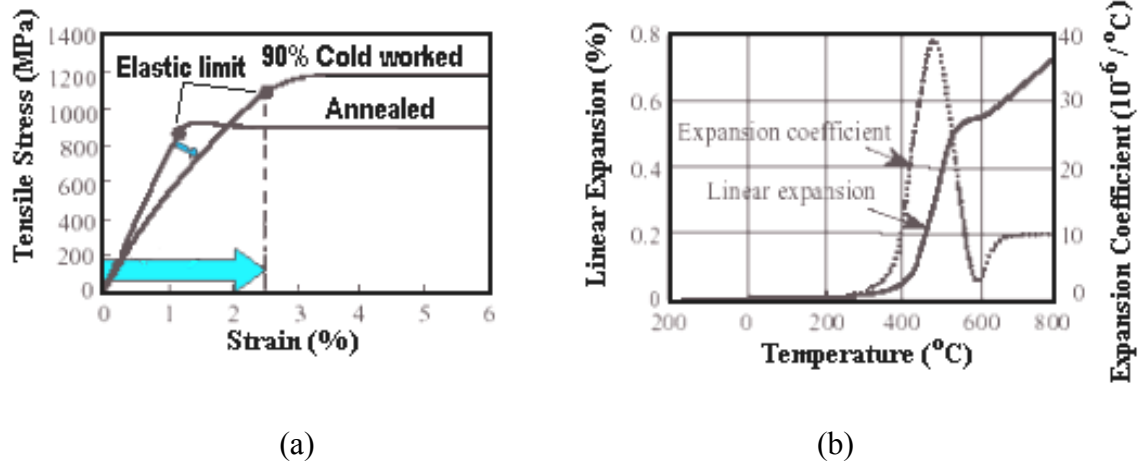
(a)   (b)

Figure 16: Mechanical and thermal properties of the super alloy "gum" metal [Ref. 7]. Fig. (a) depicts the stress strain relation of the annealed and cold-worked forms of the alloy. Fig. (b) shows the thermal expansion and CTE of the cold-worked "gum" metal.
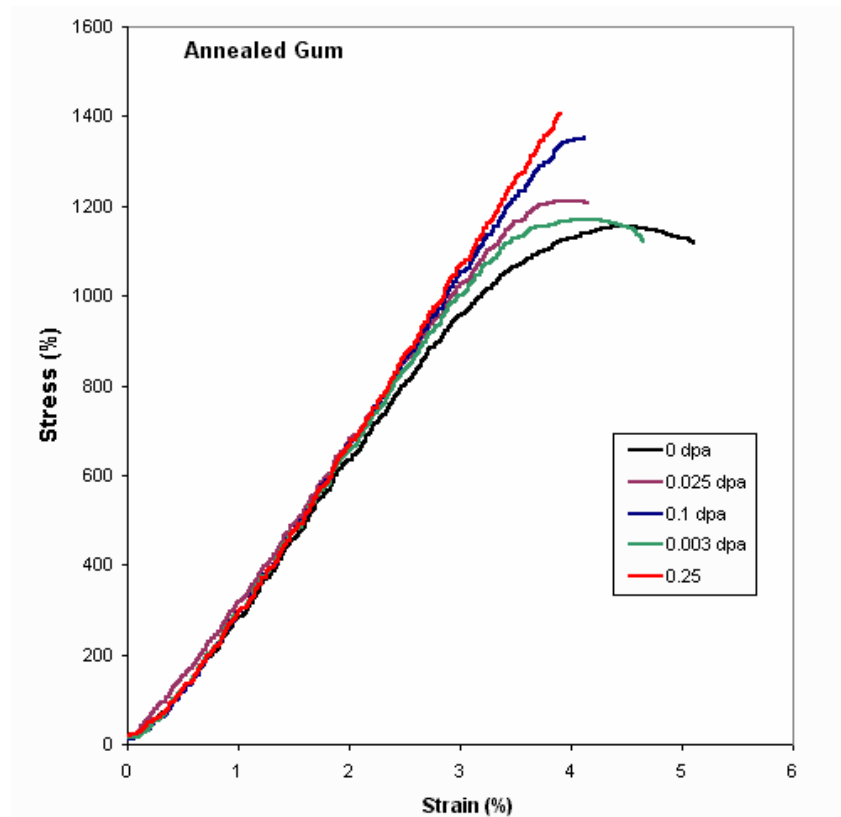

Figure 17: Irradiation effects on the stress-strain relation of the annealed gum metal. As shown, modest levels of irradiation remove the super-ductility exhibited by the alloy entirely. Note that while the elastic limit and elastic strength of the unirradiated material (0 dpa) points more towards the cold-worked material, as depicted in Fig. 16, thermal expansion analyses of the uniradiated samples confirmed that the material tested was much closer to the annealed than to the 90% cold-worked state.
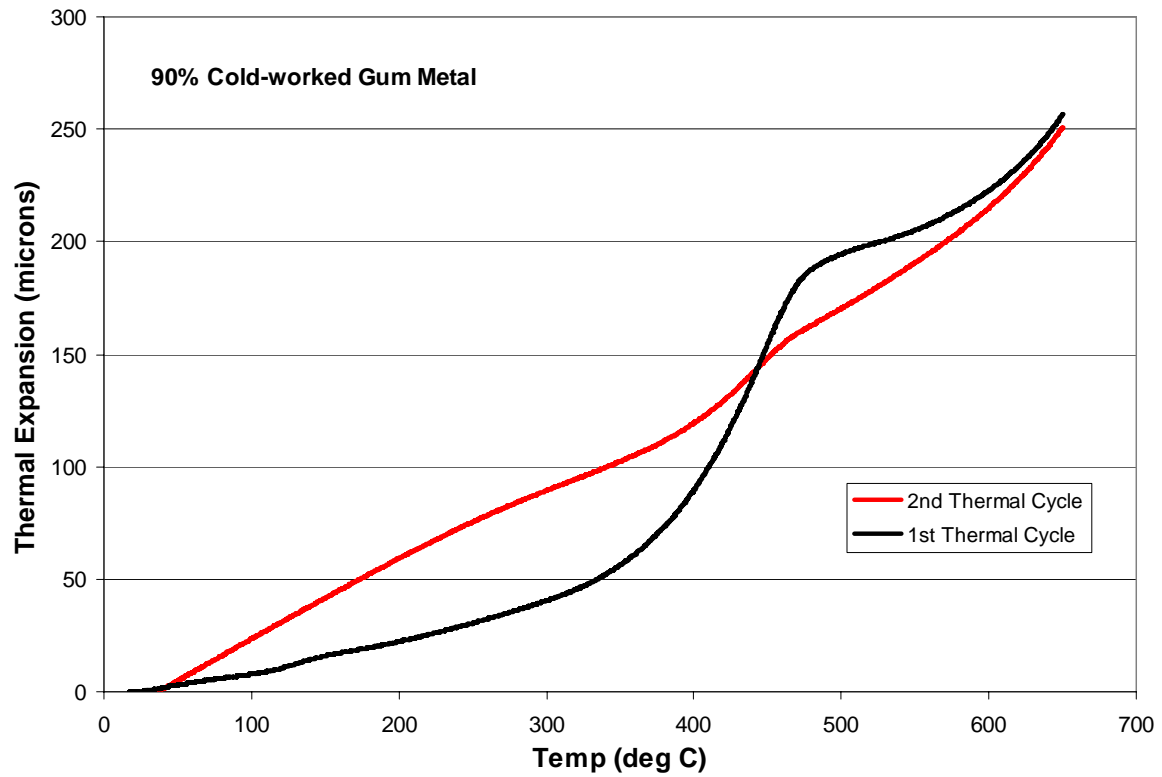
Figure 18: Effect of temperature on the invar-like properties of the cold-worked "gum" metal shown in Figure 16b. Removal of the cold-worked effects that give the alloy invar-like (or very low CTE) behavior below 400 ^{o}C and the "spike" in the range of 400-500 ^{o}C occurs with a single thermal cycle whose peak temperature exceeds 500 ^{o}C.